SPECIAL COLLECTIONS

Explore your special interest

Each issue of *CCS Chemistry* covers a wide range of research topics, and in order to help our readers browse articles of interest in their specific research area, we have created thematic Special Collections. Our virtual Special Collections cover some of our most popular topics, as well as research contributions celebrating important milestones. Our collections will allow experienced researchers to quickly view a selection of research in a particular field of interest. They also provide a survey of excellent research for those new to a field. All of our Special Collections can be viewed at:
https://www.chinesechemsoc.org/journal/ccschem/articlecollection

AUTHOR SPOTLIGHT SERIES

Meet the researchers behind the research

In every issue, we talk with a select group of authors to meet the researchers behind the research – their influences, challenges, and motivations. Check out their inspirational stories at:
https://www.chinesechemsoc.org/publications/ccschem/authorspotlight

CCS Chemistry

CCS Chemistry

COMMUNICATION

Received: Mar. 7, 2026 | Accepted: May 22, 2026 | Published: July 13, 2026

Engineering Cytochrome *c* to Catalyze Enantioselective C-Ge Bond Formation

Yangliu Feng[1†], Shao-Wu Liu[2†], Zhicong He[3†], Xiao Han[4†], Li-Qing Ren[2], Liu Yang[1], Wei Peng[1*], Chuan He[2*], Xingwang Zhang[1,5*] & Shengying Li[1,6*]

[1]*State Key Laboratory of Microbial Technology, Shandong University, Qingdao, Shandong 266237,* [2]*Shenzhen Grubbs Institute and Department of Chemistry, Guangdong Provincial Key Laboratory of Catalysis, Southern University of Science and Technology, Shenzhen, Guangdong 518055,* [3]*School of Water and Environment, Chang'an University, Xi'an, Shaanxi 710061,* [4]*College of Chemistry and Chemical Engineering, Ocean University of China, Qingdao, Shandong 266100,* [5]*Shandong Research Institute of Industrial Technology, Jinan, Shandong 250101,* [6]*Laboratory for Marine Biology and Biotechnology, Qingdao Marine Science and Technology Center, Qingdao, Shandong 266237*

**Corresponding authors:* lishengying@sdu.edu.cn; zhangxingwang@sdu.edu.cn; weipeng@sdu.edu.cn; hec@sustech.edu.cn; †Y. Feng, S.-W. Liu, Z. He, and X. Han contributed equally to this work.

Cite this: *CCS Chem.* **2026**, 8, 4365–4373
DOI: 10.31635/ccschem.026.202607664

The elemental scope of biocatalysts is far more limited than that of chemocatalysts. To date, no natural enzyme has been identified to catalyze carbon–metal bond formation, although several repurposed enzymes have been shown to facilitate non-natural C-Si and C-B bond formation. As part of our ongoing research to expand the elemental space of enzymes through the "Element Engineering" strategy, we have developed a microbial cytochrome *c*-derived mutant that can enantioselectively build C-Ge bonds both in vitro and in vivo. The mutant RccGe, obtained through two rounds of site-directed mutagenesis, exhibited a 30-fold increase in catalytic activity relative to the wild-type enzyme and produced organogermanium compounds in optically pure form. RccGe also demonstrated a broad substrate scope, accepting a wide range of germane and diazo substrates with high catalytic efficiency and stereoselectivity. Theoretical calculations revealed that the enhanced efficiency of RccGe arose from its ability to remodel the substrate-binding pocket, thereby stabilizing substrate conformations and reducing the C-to-Ge distance. This geometric preorganization effectively lowered the energy barrier for the hydrogen-atom transfer step associated with C-Ge bond formation. Overall, this study expands the elemental space accessible to natural enzymes and lays the foundation for utilizing them to synthesize organometallic compounds.

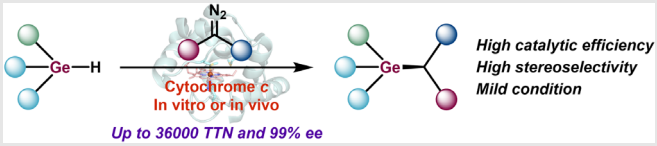

Keywords: biocatalysis, hemoprotein, enzyme engineering, carbene transfer, organogermanium compound, C-Ge bond formation

Introduction

Life originated from the combination of carbon and other chemical elements readily available on early Earth, with diverse life forms emerging as evolving "elemental assemblages" shaped by continuous interactions with the ever-changing environments.[1-3] Over billions of years of natural selection, modern life utilizes only a small subset of chemical elements for its metabolic processes. This makes the elemental scope of biocatalysts far more

limited than that of chemocatalysts. Beyond common elements such as O, N, S, and P, previous studies have uncovered natural enzymes capable of facilitating C-Se, C-As, and C-F bond formation.[4–7] Furthermore, pioneering enzyme engineering efforts have enabled enzymatic assembly of C-Si and C-B bonds.[8,9] These findings have significantly broadened the elemental scope of natural and repurposed enzymes. However, to the best of our knowledge, none of the naturally occurring enzymes have been discovered to be capable of catalyzing the bond formation between carbon and any metal element, leaving metals as a "forbidden zone" in the biosynthesis of organometallic compounds.

In 2016, Arnold and coworkers[8] first reported the use of natural hemoproteins to catalyze C-Si bond formation via carbene transfer, introducing silicon into bioorganic molecules. Germanium (Ge), the heavier congener of Si, shares the valence and bonding patterns with Si, while exhibiting stronger metallic characteristics.[10,11] Previous studies have shown that substituting carbon or silicon with germanium could fine-tune the bioactivity and other pharmacological properties of the resulting molecules (Figure 1a).[12] As a result, organogermanium compounds have been emerging as promising therapeutic agents and synthetic tools in drug discovery and molecular innovation.[12,13] Germanium possesses several distinct properties compared to carbon and silicon, including the larger atomic radius, longer C-Ge bond, stronger reducibility, and a propensity to form hypercoordinated species. These characteristics give rise to increased steric hindrance, poor stereodiscrimination, and incompatibility with standard reaction conditions. Consequently, the chemical synthesis of chiral organogermanium compounds remains highly challenging, despite recent successes such as the rhodium- and copper-based catalysts developed by the Zhou[14,15] and He groups,[16–18] respectively (Figure 1b,c). Theoretically, enzymes, benefiting from their precisely organized active sites, inherent conformational flexibility, and adaptable microenvironments, may be particularly well-suited to accommodate the distinct physicochemical properties of Ge.

Inspired by these advances and as part of our ongoing efforts to broaden the elemental space of enzymes via the "Element Engineering" strategy,[19,20] herein, we report an enzymatic approach for enantioselective C-Ge bond formation through carbene transfer using an engineered microbial cytochrome *c* (Figure 1d). Through two rounds of site-directed mutagenesis, the resulting mutant RccGe reached a total turnover number (TTN) of 36,000 with an enantiomeric excess (ee) of 99%. This work pioneers the integration of a metallic element, germanium, into the biological machinery of natural life, unlocking the potential to harness biocatalytic systems for the synthesis of organometallic compounds.

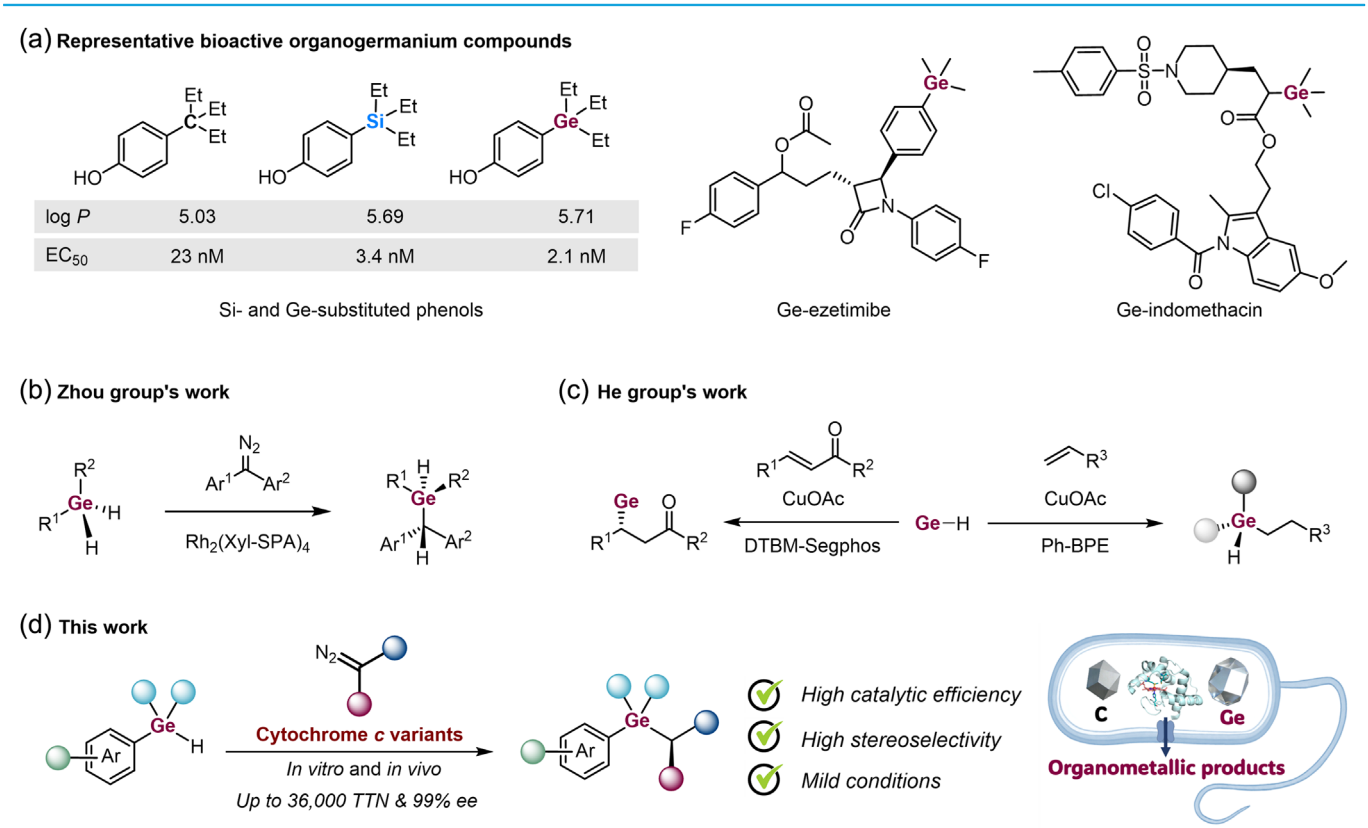

Figure 1 | *Representative organogermanium compounds and their (bio)synthetic approaches.*

DOI: 10.31635/ccschem.026.202607664
Citation: *CCS Chem.* **2026**, 8, 4365–4373
Link to VoR: https://doi.org/10.31635/ccschem.026.202607664

Results and Discussion

Hemoproteins have demonstrated great potential in mediating carbene transfer reactions in previous studies.[21–23] To investigate the ability of hemoproteins to mediate C-Ge bond formation via carbene transfer, we selected several P450 enzymes, including Cxm5,[24] PikC,[25] and P450 BM3-F87A,[26] along with a range of histidine-ligated hemoproteins for initial screening. The latter group comprised cytochrome *c* from the thermohalophilic bacterium *Rhodothermus marinus* (*Rma* cyt *c*),[8] *t*-anethole oxygenase (TAO) from *Stenotrophomonas maltophilia*,[27] and indoleamine 2,3-dioxygenase 1 (IDO1) from *Rattus norvegicus*,[28] as well as cytochrome P411 variant containing the *Bacillus subtilis* β-subunit (P411-Bsβ) and cytochrome P411 variant containing OleT from *Jeotgalicoccus* species (P411-OleT) (Figure 2b). P411-Bsβ and P411-OleT were

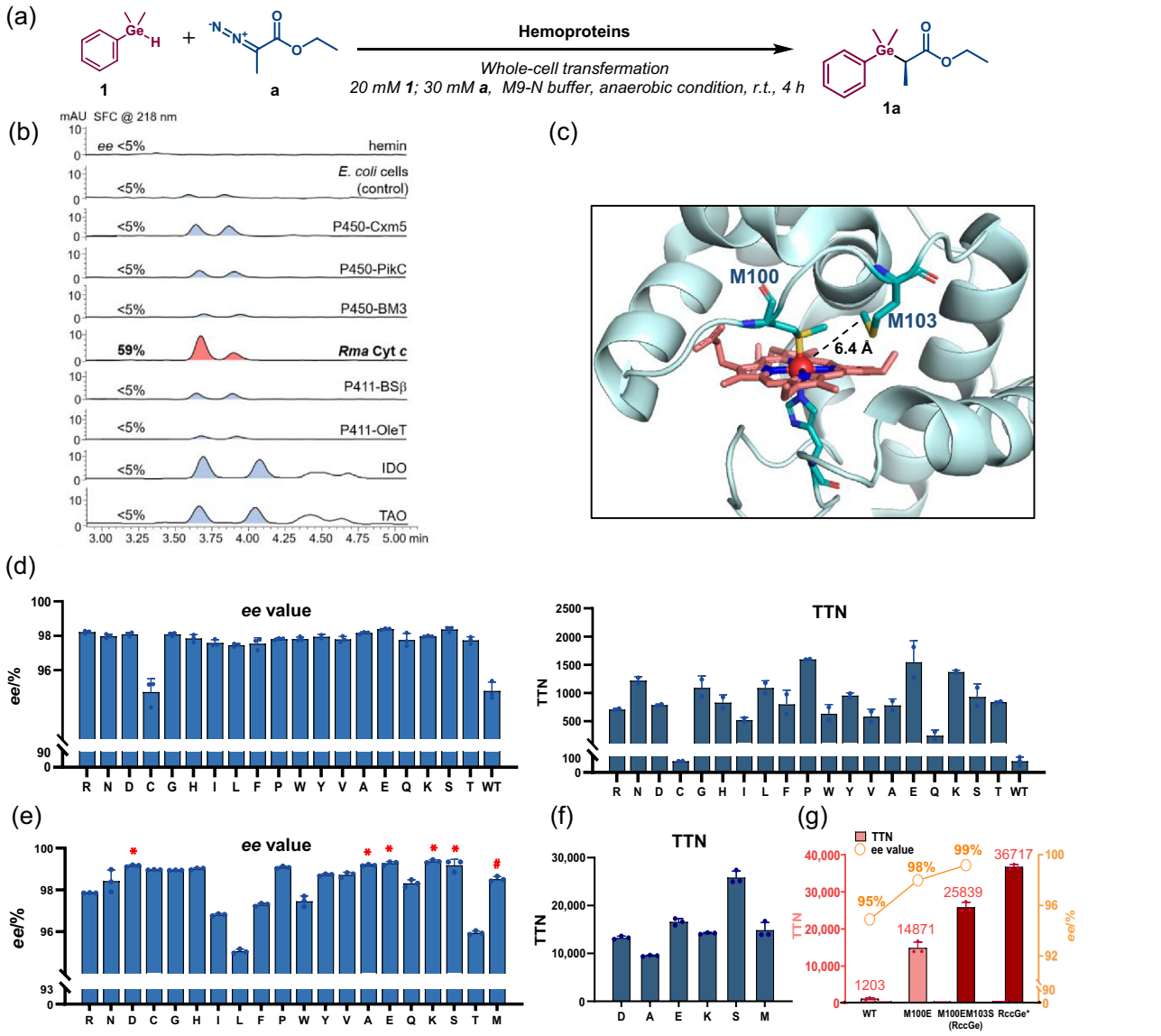

Figure 2 | *Screening and engineering of biocatalysts for C-Ge bond formation. (a) The C-Ge bond-forming reaction scheme; (b) Initial screening of hemoproteins to catalyze the carbene transfer reaction (with free hemin and* E. coli *cells without overexpressing exogenous hemoproteins as controls; detected by chiral SFC); (c) The catalytic pocket of Rma cyt c, with the mutated residues labeled; (d) The ee values and TTNs of the first-round mutants resulted from M100 saturation mutagenesis of Rma cyt c; (e) The ee values of the second-round mutants derived from M103 saturation mutagenesis of Rma cyt c-M100E (*: top five mutants by ee; #: the starting protein Rma cyt c-M100E); (f) The TTNs of the selected second-round mutants with high ee values; (g) Improvement of catalytic efficiency and enantioselectivity through two rounds of mutagenesis. RccGe*: The improved TTNs resulted from the addition of 20% (v/v) EtOH in the whole-cell reaction systems.*

DOI: 10.31635/ccschem.026.202607664
Citation: *CCS Chem.* **2026**, 8, 4365–4373
Link to VoR: https://doi.org/10.31635/ccschem.026.202607664

engineered via Cys→Ser axial heme mutations from the P450 peroxygenases $P450_{Bs\beta}$ of *Bacillus subtilis* and $OleT_{JE}$ of *Jeotgalicoccus* species from the American Type Culture Collection under accession number 8456 (ATCC 8456), respectively (Supporting Information Tables S1–S3).[29,30]

These hemoproteins were individually expressed in *Escherichia* (*E.*) *coli* BL21(DE3) with an *N*-terminal His_6- or engineered small ubiquitin-like modifier fusion tag variant (SUMO-His_6-tag). By nickel-nitrilotriacetic acid (Ni-NTA) affinity chromatography and sodium dodecyl sulfate–polyacrylamide gel electrophoresis (SDS-PAGE) analysis, all proteins were confirmed to be solubly expressed and purified (Supporting Information Figure S1). Subsequently, we evaluated these hemoproteins for their ability to catalyze the Ge-H carbene insertion. The assays were performed using a whole-cell transformation system (OD_{600} = 60) at room temperature under anaerobic conditions for 4 h, with dimethylphenylgermane (**1**, 20 mM) and ethyl 2-diazopropionate (**a**, 30 mM) as carbene precursor (Figure 2a). Supercritical fluid chromatography–mass spectrometry (SFC-MS) and gas chromatography–mass spectrometry (GC-MS) analyses showed that all the tested proteins were able to mediate C-Ge bond formation to yield product **1a** (Figure 2b and Supporting Information Figure S2). However, only *Rma* cyt *c* generated the product in an enantioselective manner (Figure 2b). Notably, we found that *E. coli* cells without overexpressing exogenous hemoproteins also produced a small amount of **1a**, likely due to the activity of its endogenous hemoproteins. In addition, a control reaction with the addition of free hemin produced a trace amount of **1a**, only detectable by MS analysis. Consequently, we selected *Rma* cyt *c* as the starting protein for further engineering in order to enhance its catalytic efficiency and enantioselectivity.

Given that cytochrome *c* requires complex post-translational modifications in vivo to reach maturity and be transported to the periplasmic space,[31,32] we turned to express it in *Pseudomonas fluorescens*, which possesses a more efficient protein post-translational modification processing system.[20] Protein purification and SDS-PAGE analysis confirmed its soluble expression in this host (Supporting Information Figure S1). The concentrations of *Rma* cyt *c* in whole cells and cell lysates were determined using the pyridine hemochrome method.[33] Activity assays showed that whole-cell catalysis was more efficient, likely because the diazo substrate could inhibit cytochrome *c* in cell lysates. In contrast, cell lysates exhibited greater stereoselectivity, likely due to heat inactivation of endogenous nonselective hemoproteins (Supporting Information Figure S3). Taken together, we established a standard reaction setup for the C-Ge formation assay as follows: using a biocatalyst loading of 0.007 mol % (i.e., 1.4 μM *Rma* cyt *c*, 20 mM **1**, and 30 mM **a**), the wild-type hemoprotein produced **1a** with a TTN of 1,203 and 90% ee in whole-cell transformation, and with a TTN of 79 and 95% ee in the lysate-based reaction. These results provided a starting point for the subsequent engineering efforts.

According to previous studies, mutation of the M100 residue in *Rma* cyt *c*, which coordinates the distal heme iron, facilitated carbene transfer reactions (Figure 2c).[8] Thus, we performed saturation mutagenesis at M100 using combined degenerate primers and site-directed mutagenesis. Activity assays using each cell lysate of the 19 resulting mutants revealed that nearly all variants exhibited higher catalytic efficiency and enantioselectivity than the wild-type (Figure 2d). Among these, the M100E mutant, which demonstrated the highest efficiency and enantioselectivity, was selected for further engineering. A total of 10 mg of product **1a** was obtained through whole-cell transformation using the M100E mutant, followed by purification via chiral high-performance liquid chromatography (HPLC). Its structure was determined by nuclear magnetic resonance (NMR) analysis (Supporting Information Figures S4–S8), and its absolute configuration was assigned as *R* by comparing the experimental circular dichroism (CD) spectrum with the calculated electronic circular dichroism (ECD) spectrum (Supporting Information Figure S9). Quantitative analysis revealed that the M100E mutant reached an ee of 98% and a TTN of 1,543 in lysate reaction, and an ee of 98% and a TTN of 14,871 in whole-cell transformation (Figure 2g).

Structural analysis of *Rma* cyt *c* revealed that residue M103, situated within the substrate access channel and in proximity to the heme-Fe center (6.4 Å), likely played an important role in modulating the catalytic properties (Figure 2c). Therefore, we selected the M103 residue for a second round of saturation mutagenesis. We first determined the stereoselectivity of the resulting 19 mutants using cell lysates. As a result, 11 mutants displayed improved ee values over the starting protein (Figure 2e). Next, the five mutants with the highest ee values (M103D, M103A, M103E, M103K, and M103S) were tested for their catalytic efficiency via whole-cell transformation, and M103S demonstrated the highest catalytic efficiency with a TTN of 25,839 (Figure 2f). Since substrate **1** had low solubility in water, we then added 20% (v/v) ethanol as a cosolvent to promote the reaction. As expected, this adjustment further increased the TTN of the M100E-M103S mutant to 36,717 in a whole-cell manner. Taken together, through two rounds of site-directed saturation mutagenesis, we obtained the high-performance mutant *Rma* cyt *c* M100E-M103S (RccGe) for enantioselective C-Ge bond formation. Its TTN was 30 times greater than that of the wild-type enzyme, and it exhibited an ee value of 99% (Figure 2g).

Next, we investigated the substrate scope of RccGe. Cell lysates of *P. fluorescens* expressing RccGe were coincubated with a range of germane reagents (**2**–**10**) and diazo reagents (**b**–**d**) (Supporting Information

DOI: 10.31635/ccschem.026.202607664
Citation: *CCS Chem.* **2026**, 8, 4365–4373
Link to VoR: https://doi.org/10.31635/ccschem.026.202607664

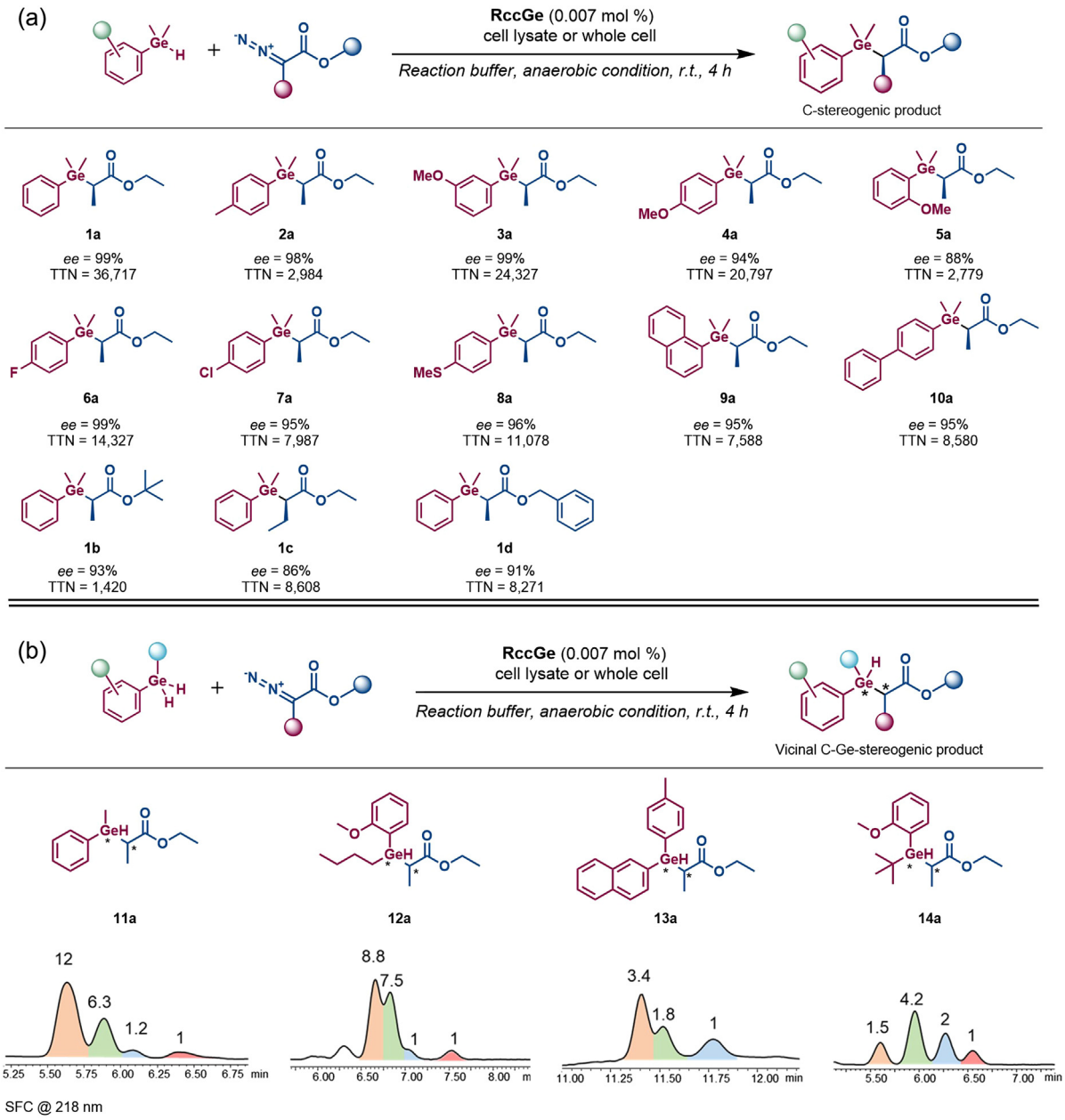

Figure 3 | *Substrate scope of RccGe. (a) C-stereogenic products; (b) Vicinal C-Ge-stereogenic products (The numbers above the peaks indicate the relative ratios).*

Figures S10 and S122–S145). GC-MS and SFC-MS analyses showed that RccGe was able to catalyze the carbene transfer reactions between all tested germane and diazo reagents (Figure 3a and Supporting Information Figures S11–S22). We prepared all the products by whole-cell transformations and chiral HPLC, with their structures confirmed by NMR analysis (Supporting Information Figures S10 and S23–S95). Comparisons of the CD and ECD spectra confirmed that all these products possessed an *R*-configured stereocenter (Figure 3a and Supporting Information Figure S9). As calculated, most reactions exhibited ee values exceeding 90% (Figure 3a and Supporting Information Figures S96–S108). These results demonstrate that RccGe accepted both electron-rich and electron-deficient germanane substrates bearing substitutions at different positions (**1**–**8**), as well as bulky naphthyl- and biphenyl-substituted germananes (**9**–**10**), while maintaining high enantioselectivity (Figure 3a). The diazo reagents, replacing the ethyl ester with bulkier *tert*-butyl (**1b**), benzyl (**1d**) esters, and the methyl with a bulkier ethyl group (**1c**), were all tolerated by RccGe catalysis (Figure 3a).

To further assess the ability of RccGe to control stereochemistry at the vicinal *bis*-Ge-C stereogenic centers,

DOI: 10.31635/ccschem.026.202607664
Citation: *CCS Chem.* **2026**, 8, 4365–4373
Link to VoR: https://doi.org/10.31635/ccschem.026.202607664

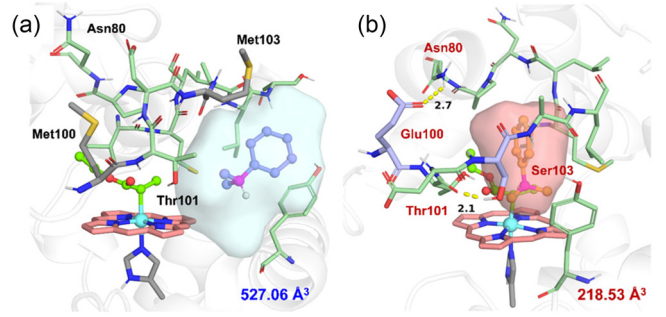

Figure 4 | *Substrate-binding pockets of Rma cyt c and RccGe. (a) The substrate-binding pocket of Rma cyt c is shown in light blue, with surrounding amino acid residues in green. Key mutation sites M100 and M103 are highlighted in gray. (b) The substrate-binding pocket of RccGe is shown in light red, with mutated residues E100 and S103 highlighted in purple. In this variant, E100 and S103 form a hydrogen bond with N80 and T101, respectively.*

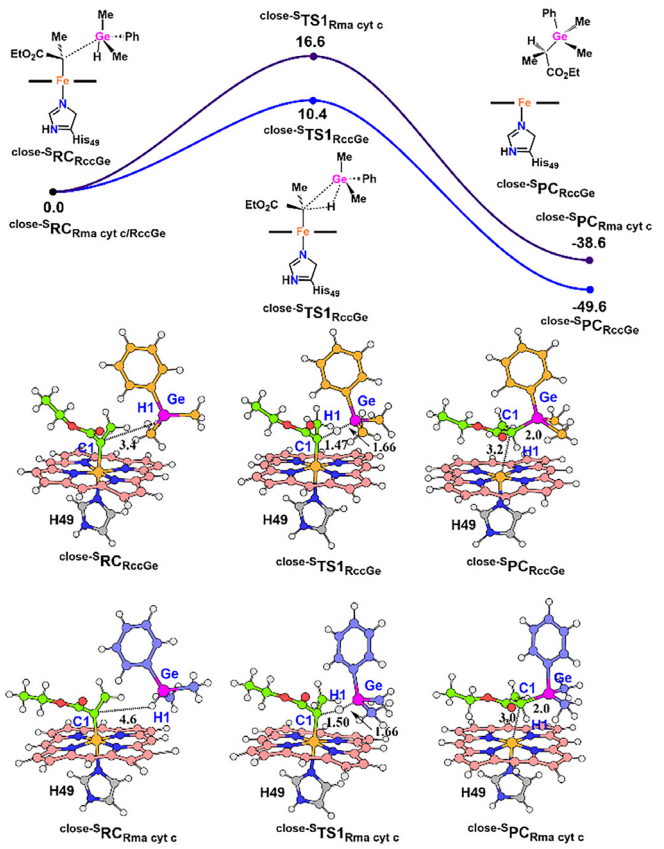

Figure 5 | *QM(UB3LYP-D3/B2)/MM-calculated reaction mechanism for C-Ge bond formation catalyzed by Rma cyt c and RccGe (with energies in kcal/mol). Key interatomic distances are given in angstroms (Å); The QM/MM-optimized structures of the key reaction species are also presented. The cosubstrate **1** is marked in orange and purple for the RccGe and Rma cyt c systems, respectively.*

we designed and synthesized a series of dihydrogermane substrates (**11**–**14**) and reacted them individually with diazo reagent **a** (Figure 3b). Theoretically, four enantiomeric/diastereomeric products could be formed. As expected, GC-MS and chiral SFC-MS analysis showed that all reactions proceeded to afford all four products, which were detected in distinct isomeric ratios (Figure 3b and Supporting Information Figures S109–S116). Nevertheless, due to the difficulty in separating the products via chiral SFC or HPLC, the absolute stereochemistry of each product remained unassigned. These results nevertheless demonstrated that RccGe exhibited modest stereoselectivity toward products bearing vicinal Ge- and C-stereogenic centers. This was attributed to the relatively loose catalytic pocket of the current mutant, which accommodated multiple reactive conformations during carbene transfer to the Ge-H bond. We are currently working to engineer RccGe further to achieve precise control over the stereochemistry of such vicinal Ge- and C-stereogenic products.

To elucidate the structural and electronic origins underlying the distinct catalytic performance of *Rma* cyt *c* and RccGe, we constructed a composite model comprising the C-Fe-bonded carbene intermediate formed after N_2 extrusion from the substrate **a** in complex with the cosubstrate **1** (Supporting Information Figure S117). The binding configurations of **1** were systematically analyzed in both systems. Molecular docking (MD) clustering analysis revealed that, in *Rma* cyt *c*, the dominant binding modes of **1** were restricted to three conformational families (Supporting Information Figure S117), primarily due to pronounced steric hindrance imposed by Met100 and Met103. In a substantial fraction of these conformers, the phenyl ring of **1** is oriented toward the interior of the binding pocket. In contrast, this steric constraint was effectively relieved in RccGe, leading to a marked reorganization of the preferred binding modes, in which the phenyl group predominantly adopted an upward or outward-facing orientation. Consistent with these conformational differences, the C-Ge distances exhibited a pronounced divergence between the two systems. In *Rma* cyt *c*, the average C-Ge distance was ~8 Å (Supporting Information Figure S117), whereas in RccGe this distance is reduced to ~5 Å (Supporting Information Figure S117), indicating a substantially more favorable geometric preorganization for C-Ge bond formation. The origin of this difference in substrate proximity was traced to distinct features of the substrate-binding pocket, as revealed by reconstructed binding-site models of the *Rma* cyt *c* and RccGe (Figure 4). In RccGe, a compact substrate-binding pocket (218.5 Å^3) was stabilized by persistent hydrogen bonds between E100 and N80, and between S103 and T101, with hydrogen-bond distances remaining stable throughout the 100–200 ns MD simulations

DOI: 10.31635/ccschem.026.202607664
Citation: *CCS Chem.* **2026**, 8, 4365–4373
Link to VoR: https://doi.org/10.31635/ccschem.026.202607664

(Figure 4b and Supporting Information Figure S118). As a result, the distance from the reactive carbon atom to the center of the metal-adjacent pocket was reduced to ~5 Å(Supporting Information Figure S119). This structural constraint stabilized productive substrate conformations and positioned the Ge atom closer to the carbene. In contrast, *Rma* cyt *c* featured a significantly larger and more flexible binding pocket, with a calculated volume of 527 Å^3 (Figure 4a) and an increased carbon-to-pocket-center distance of 7.5 Å (Supporting Information Figure S119). The expanded pocket geometry likely destabilized the substrate conformation and increased the Ge-carbene bond distance, thereby disfavoring C-Ge bond formation.

Next, representative reactive conformations with short C-Ge distances were selected from both systems for quantum mechanics/molecular mechanics (QM/MM) calculations. In *Rma* cyt *c*, the open-shell singlet and closed-shell singlet reactant states are nearly isoenergetic, with an energy difference of only 0.9 kcal/mol, whereas the triplet state is thermodynamically disfavored by 14.6 kcal/mol relative to the open-shell singlet (Supporting Information Figure S120). Along the closed-shell reaction pathway, hydrogen transfer from Ge to the coordinated carbon center proceeds with an activation barrier of 16.6 kcal/mol ($RC_{Rma\ cyt\ c} \rightarrow {}^{close\text{-}S}TS1_{Rma\ cyt\ c}$), followed by concerted C-Ge bond formation to yield the product state ($^{close\text{-}S}PC_{Rma\ cyt\ c}$), accompanied by a substantial exothermicity of −38.6 kcal/mol (Figure 5). Strikingly, RccGe demonstrated significantly enhanced kinetic and thermodynamic properties via the same closed-shell reaction pathway. The barrier for the H-transfer was reduced to 10.4 kcal/mol, and the subsequent synchronous formation of the C-Ge bond led to the product state ($^{close\text{-}S}PC_{RccGe}$) with an enhanced reaction exothermicity of −49.6 kcal/mol. Notably, in the open-shell singlet manifold, both the *Rma* cyt *c* and RccGe systems stabilized only H-transferred intermediates ($^{open\text{-}S}IC1_{Rma\ cyt\ c}$ and $^{open\text{-}S}IC1_{RccGe}$), while spontaneous C-Ge bond formation was not observed. Potential energy along the C-Ge bond coordinate revealed a monotonic increase in energy upon bond contraction, excluding the open-shell pathway and establishing that the reaction proceeded intrinsically via a closed-shell mechanism.

Conclusion

Through two rounds of site-directed saturation mutagenesis for two key amino acid residues in the active site, we successfully engineered a *Rma* cyt *c* into an efficient biocatalyst RccGe. This hemoprotein was capable of enantioselectively catalyzing C-Ge bond formation both in vitro and in vivo, enabling the introduction of a metal element into a natural enzyme machinery for organometallic compound production. RccGe exhibited broad substrate scope, favoring enantioselective synthesis of organogermanium compounds toward a variety of germane and diazo reagents bearing diverse functional groups; however, further engineering work is required to enhance its stereoselectivity when handling complex vicinal *bis*-Ge-C stereogenic centers. Theoretical calculations suggested that the enhanced catalytic efficiency of RccGe, compared with the wild-type enzyme, arose from a mutation-induced hydrogen-bonding network. This network contracted the substrate-binding pocket, facilitated closer Ge-C proximity, promoting a lower activation barrier for Ge-H bond activation. During the preparation of this manuscript, the Yang group reported the C-Ge bond formation catalyzed by an artificial enzyme mutant, FeHP-1_{Ge}.[34] A comparative analysis revealed that the RccGe variant, which underwent fewer rounds of engineering than FeHP-1_{Ge}, exhibited both higher catalytic efficiency and enantioselectivity in whole-cell catalysis (Supporting Information Figure S121). Additionally, compared with the previously reported rhodium-based chemocatalyst, the present study offers a biocatalytic strategy for producing organogermanium compounds that employs an engineered cytochrome *c* as the catalytic scaffold, via a closed-shell hydrogen-atom transfer mechanism under mild aqueous conditions with an ultralow enzyme loading (0.007 mol %). Collectively, this study establishes a biocatalytic strategy for synthesizing organogermanium compounds and demonstrates that natural enzymes could catalyze bond formation between carbon and metal elements, thereby expanding the chemical and elemental space accessible to biocatalysis.

Supporting Information

Supporting Information is available and includes experimental procedures and characterization data.

Conflict of Interest

There is no conflict of interest to report.

Funding Information

This work was supported by the National Key R&D Program of China (grant no. 2023YFA0915500), the Shandong Provincial Natural Science Foundation, China (grant no. ZR2023ZD50), the National Natural Science Foundation of China (grant nos. 32470043, 22577066, and 22271134), and the Taishan Scholars Program, China (grant nos. tsqn202408318 and tsqn202507079).

Acknowledgments

We thank Xiangmei Ren, Shunni Dong, Jingyao Qu, Jing Zhu, Zhifeng Li, Guannan Lin, and Haiyan Sui from the

DOI: 10.31635/ccschem.026.202607664
Citation: *CCS Chem.* **2026**, 8, 4365–4373
Link to VoR: https://doi.org/10.31635/ccschem.026.202607664

State Key Laboratory of Microbial Technology at Shandong University, China, for their guidance and help in SFC-MS, liquid chromatography-mass spectrometry (LC-MS), GC-MS, and NMR analysis. We also thank Yanli Guo from Shimadzu China Innovation Center, Shimadzu (China) Co., Ltd., Beijing, China, for the guidance and help in SFC-MS analysis.

References

1. Broadley, M. W.; Bekaert, D. V.; Piani, L.; Füri, E.; Marty, B. Origin of Life-Forming Volatile Elements in the Inner Solar System. *Nature* **2022**, *611*, 245–255.
2. Cairns-Smith, A. G. Chemicals Unbottled. *Nature* **1996**, *383*, 310–311.
3. Williams, R. J. P. The Natural Selection of the Chemical Elements. *Cell. Mol. Life Sci.* **1997**, *53*, 816–829.
4. Hoshino, S.; Ijichi, S.; Asamizu, S.; Onaka, H. Insights into Arsenic Secondary Metabolism in Actinomycetes from the Structure and Biosynthesis of Bisenarsan. *J. Am. Chem. Soc.* **2023**, *145*, 17863–17871.
5. Kayrouz, C. M.; Huang, J.; Hauser, N.; Seyedsayamdost, M. R. Biosynthesis of Selenium-Containing Small Molecules in Diverse Microorganisms. *Nature* **2022**, *610*, 199–204.
6. Kayrouz, C. M.; Ireland, K. A.; Ying, V. Y.; Davis, K. M.; Seyedsayamdost, M. R. Discovery of the Selenium-Containing Antioxidant Ovoselenol Derived from Convergent Evolution. *Nat. Chem.* **2024**, *16*, 1868–1875.
7. Dong, C. J.; Huang, F. L.; Deng, H.; Schaffrath, C.; Spencer, J. B.; O'Hagan, D.; Naismith, J. H. Crystal Structure and Mechanism of a Bacterial Fluorinating Enzyme. *Nature* **2004**, *427*, 561–565.
8. Kan, S. B. J.; Lewis, R. D.; Chen, K.; Arnold, F. H. Directed Evolution of Cytochrome *c* for Carbon-Silicon Bond Formation: Bringing Silicon to Life. *Science* **2016**, *354*, 1048–1051.
9. Kan, S. B. J.; Huang, X. Y.; Gumulya, Y.; Chen, K.; Arnold, F. H. Genetically Programmed Chiral Organoborane Synthesis. *Nature* **2017**, *552*, 132–136.
10. Guselnikova, T. Y. History and Recent Advances in Elemental Analysis of Germanium-Based Functional Materials. *Talanta* **2023**, *251*, 123792.
11. Narokha, V.; Nizhenkovska, I.; Kuznetsova, O. Potential of Germanium-Based Compounds in Coronavirus Infection. *Acta Pharm.* **2022**, *72*, 245–258.
12. Xu, M. Y.; Li, N.; Xiao, B. Recently Developed Organogermanium(IV) Compounds as Drug Candidates and Synthetic Tools in Drug Discovery. *Org. Biomol. Chem.* **2025**, *23*, 7852–7871.
13. Luo, X.; Sun, J.; Kong, D.; Lei, Y.; Gong, F.; Zhang, T.; Shen, Z.; Wang, K.; Luo, H.; Xu, Y. The Role of Germanium in Diseases: Exploring Its Important Biological Effects. *J. Transl. Med.* **2023**, *21*, 795.
14. Han, A. C.; Xiao, L. J.; Zhou, Q. L. Construction of Ge-Stereogenic Center by Desymmetric Carbene Insertion of Dihydrogermanes. *J. Am. Chem. Soc.* **2024**, *146*, 5643–5649.
15. Han, A.-C.; Zhang, X.-G.; Yang, L.-L.; Pan, J.-B.; Zou, H.-N.; Li, M.-L.; Xiao, L.-J.; Zhou, Q.-L. Rhodium-Catalyzed Enantioselective C–Ge Bond Formation by Carbene Insertion: Efficient Access to Chiral Organogermanes. *Chem Catal.* **2024**, *4*, 100826.
16. Lin, W.; Ren, L.-Q.; Du Chen, C.; Han, X.; Zhang, L.; Chen, Z.; Guo, J.; He, C. Cu-Catalyzed Asymmetric Hydrogermylation Towards C- and Ge-Stereogenic Germanes. *CCS Chem.* **2025**, *7*, 1157–1167.
17. Lin, W.; You, L.; Yuan, W.; He, C. Cu-Catalyzed Enantioselective Hydrogermylation: Asymmetric Synthesis of Unnatural β-Germyl α-Amino Acids. *ACS Catal.* **2022**, *12*, 14592–14600.
18. Liu, S.-W.; Ke, J.; He, C. Recent Advances in Catalytic Asymmetric Synthesis of Chiral Organogermanes. *Chiral Chem.* **2026**, *2*, 202601.
19. Zhang, X. W.; Cheng, F. Y.; Guo, J. W.; Zheng, S. M.; Wang, X.; Li, S. Y. Enzymatic Synthesis of Organoselenium Compounds via C–Se Bond Formation Mediated by Sulfur Carrier Proteins. *Nat. Synth.* **2024**, *3*, 477–487.
20. Wang, X.; Tian, X.; Guo, J.; Cheng, F.; Liu, M.; Zheng, S.; Feng, Y.; Lv, Y.; Li, Y.; Li, S.; Zhang, X. Carboxylic Acid Tailoring in Thioquinolobactin Biosynthesis. *J. Nat. Prod.* **2025**, *88*, 1425–1433.
21. Yang, Y.; Arnold, F. H. Navigating the Unnatural Reaction Space: Directed Evolution of Heme Proteins for Selective Carbene and Nitrene Transfer. *Acc. Chem. Res.* **2021**, *54*, 1209–1225.
22. Brandenberg, O. F.; Fasan, R.; Arnold, F. H. Exploiting and Engineering Hemoproteins for Abiological Carbene and Nitrene Transfer Reactions. *Curr. Opin. Biotechnol.* **2017**, *47*, 102–111.
23. Zhang, R. K.; Huang, X.; Arnold, F. H. Selective C–H Bond Functionalization with Engineered Heme Proteins: New Tools to Generate Complexity. *Curr. Opin. Chem. Biol.* **2019**, *49*, 67–75.
24. Zhang, X.; Xu, X.; You, C.; Yang, C.; Guo, J.; Sang, M.; Geng, C.; Cheng, F.; Du, L.; Shen, Y.; Wang, S.; Lan, H.; Yang, F.; Li, Y.; Tang, Y. J.; Zhang, Y.; Bian, X.; Li, S.; Zhang, W. Biosynthesis of Chuangxinmycin Featuring a Deubiquitinase-Like Sulfurtransferase. *Angew. Chem. Int. Ed.* **2021**, *60*, 24418–24423.
25. Sherman, D. H.; Li, S.; Yermalitskaya, L. V.; Kim, Y.; Smith, J. A.; Waterman, M. R.; Podust, L. M. The Structural Basis for Substrate Anchoring, Active Site Selectivity, and Product Formation by P450 PikC from *Streptomyces venezuelae*. *J. Biol. Chem.* **2006**, *281*, 26289–26297.
26. Munro, A. W.; Leys, D. G.; McLean, K. J.; Marshall, K. R.; Ost, T. W.; Daff, S.; Miles, C. S.; Chapman, S. K.; Lysek, D. A.; Moser, C. C.; Page, C. C.; Dutton, P. L. P450 BM3: The Very Model of a Modern Flavocytochrome. *Trends Biochem. Sci.* **2002**, *27*, 250–257.
27. Purwani, N. N.; Rozeboom, H. J.; Willers, V. P.; Wijma, H. J.; Fraaije, M. W. Discovery of a New Class of Bacterial Heme-Containing C=C Cleaving Oxygenases. *New Biotechnol.* **2024**, *83*, 82–90.

DOI: 10.31635/ccschem.026.202607664
Citation: *CCS Chem.* **2026**, 8, 4365–4373
Link to VoR: https://doi.org/10.31635/ccschem.026.202607664

28. Nori, P.; Haghshenas, R.; Aftabi, Y.; Akbari, H. Comparison of Moderate-Intensity Continuous Training and High-Intensity Interval Training Effects on the IDO1-KYN-Ahr Axis in the Heart Tissue of Rats with Occlusion of the Left Anterior Descending Artery. *Sci. Rep.* **2023**, *13*, 3721.
29. Liu, Y.; Wang, C.; Yan, J.; Zhang, W.; Guan, W.; Lu, X.; Li, S. Hydrogen Peroxide-Independent Production of Alpha-Alkenes by OleTJE P450 Fatty Acid Decarboxylase. *Biotechnol. Biofuels* **2014**, *7*, 28.
30. Hyster, T. K.; Arnold, F. H. P450BM3-Axial Mutations: A Gateway to Non-Natural Reactivity. *Isr. J. Chem.* **2014**, *55*, 14–20.
31. Das, T. K.; Pecoraro, C.; Tomson, F. L.; Gennis, R. B.; Rousseau, D. L. The Post-Translational Modification in Cytochrome *c* Oxidase is Required to Establish a Functional Environment of the Catalytic Site. *Biochemistry* **1998**, *37*, 14471–14476.
32. Kranz Robert, G.; Richard-Fogal, C.; Taylor, J.-S.; Frawley Elaine, R. Cytochrome *c* Biogenesis: Mechanisms for Covalent Modifications and Trafficking of Heme and for Heme-Iron Redox Control. *Microbiol. Mol. Biol. Rev.* **2009**, *73*, 510–528.
33. Barr, I.; Guo, F. Pyridine Hemochromagen Assay for Determining the Concentration of Heme in Purified Protein Solutions. *Bio. Protoc.* **2015**, *5*, e1594.
34. Huang, W.; Adornato, G. M.; Horst, M.; Alturaifi, T. M.; Hou, K.; Liu, P.; DeGrado, W. F.; Yang, Y. De Novo Design, Directed Evolution and Computational Study of Heme-Binding Helical Bundle Protein Catalysts for Biocatalytic Enantioselective Ge-H Insertion. *J. Am. Chem. Soc.* **2025**, *147*, 40869–40878.

DOI: 10.31635/ccschem.026.202607664
Citation: *CCS Chem.* **2026**, 8, 4365–4373
Link to VoR: https://doi.org/10.31635/ccschem.026.202607664